FLUORESCENCE PHOTOBLEACHING RECOVERY IN SOLUTIONS OF LABELED ACTIN

FREDERICK LANNI, *Biophysics Program, Harvard University, Cambridge, Massachusetts 02138*
D. LANSING TAYLOR, *Cell and Developmental Biology, Harvard University, Cambridge, Massachusetts 02138*
B. R. WARE, *Department of Chemistry, Syracuse University, Syracuse, New York 13210*

ABSTRACT We have demonstrated that the technique of fluorescence photobleaching recovery (FPR) can be used to examine the state of a single component in complex self-assembling macromolecular systems. Polymerization of actin, initiated by addition of salt or Mg^{+2} to a low-ionic-strength solution of G-actin, has been observed by sequential measurement of FPR with the aid of fluorescein-labeled actin. Solutions of actin which had been labeled using 5-iodoacetamido fluorescein (5-IAF) showed anomalous recovery of fluorescence above the initial value, which indicates a photoinduced increase in local polymerization. No such anomaly was observed with actin that had been labeled with fluorescein isothiocyanate (FITC). The FPR data are directly interpretable in terms of the fraction of labeled protein that is immobilized in the supramolecular assembly and in terms of the average diffusion coefficient of the mobile fraction. Our data are consistent with the "treadmill" model of actin polymerization, in that they show that actin is present under polymerizing conditions either as a high polymer or as monomer or low oligomer. We believe that the FPR technique can be applied to the study of many types of reconstituted motile or cytoskeletal systems in vitro or in vivo.

INTRODUCTION

Biophysical models of cell motility must explain the nature and control of actin filament formation and degradation. Viscometry (1–5), light scattering spectroscopy (6, 7), electron microscopy (8–10), and the tracer methods of fluorescence (11–14), spin resonance (15, 16), and radioactivity (17) have been used to study actin and other components of the cytoskeleton and contractile apparatus. Viscometry has been the classical method for the study of solutions of actin because the formation of filaments has a large effect upon the rheological properties of the solution. The viscosity of a dilute solution of actin is mainly a measure of the amount of long filamentous actin present, and is a relatively insensitive function of the amount of G-actin and smaller filaments. More concentrated solutions of actin are viscoelastic and undergo irreversible changes in response to mechanical stress. Although viscosity is a good indicator of filament formation, and has been used successfully to identify actin-binding proteins, it is not a quantity suitable to characterize viscoelastic systems (18).

We report here that the polymerization of G-actin into filaments can be observed by measuring fluorescence photobleaching recovery (FPR) in solutions of actin in which actin has been covalently labeled with a fluorophore. Each fluorescence photobleaching recovery record is a measure of the distribution of the label over a range of mobility; the slow

components of the recovery are due to long actin filaments having a low diffusion coefficient, and the rapid components of the recovery are due to actin monomers and oligomers. Measurement of FPR therefore has the potential to yield more detailed information about actin filament formation than measurement of viscosity, without subjecting the solution to mechanical stress.

THEORY

Measurement of fluorescence photobleaching recovery, as described by Peters et al. (19), Jacobson et al. (20), and Axelrod et al. (21), allows determination of the mobility of particles large enough that attachment of a fluorophore does not significantly alter the motion of the particles. In the FPR method, a brief, intense pattern of illumination is used to create a detectable concentration profile in an initially homogenous distribution of fluorescent label by a photochemical bleaching reaction, without affecting the distribution of the carrier particles. The bleached pattern is monitored by using a much lower illumination intensity to excite fluorescent emission. In the absence of sedimentation, convection, active transport, or other forms of directed flow, dissipation of the bleached pattern occurs because of thermal motion (diffusion) of the labeled particles. Fluorescence recovery occurs as unbleached particles from outside the illuminated region replace bleached particles that diffuse away. Since the initial homogeneous distribution of particles is unaffected by photobleaching, the fluorescence recovery is an explicit function of the tracer diffusion coefficient of the particles.

In our experiments, fluorescence recoveries are observed after photobleaching a small volume in a homogeneous solution of labeled protein. Because particle mobility in solution is unconstrained (three-dimensional), the relation between the diffusion coefficient and the orientationally averaged frictional coefficient of the labeled particles is strictly defined by Einstein's relation: $D = kT/f$. The frictional coefficient can be related to the dimensions of the diffusing particle if its general shape is known. The usefulness of the FPR method for the rapid determination of protein diffusion coefficients has been demonstrated by Barisas and Leuther (22).

The incorporation of labeled G-actin into filaments produces a distribution of particles labeled in proportion to their length. Because of the distribution of particle size, the fluorescence recovery will not be a function of a single diffusion coefficient, but must be expressed as a weighted sum or integral:

$$i_F(t) = \int_0^{D_0} i_F(t, D)\, f_F(D)\, \mathrm{d}D. \tag{1}$$

Here $i_F(t, D)$ is the recovery which would be observed because of a single molecular species with diffusion coefficient D, and $f_F(D)$ is the normalized distribution of fluorescence as a function of D. The major problem in the analysis of FPR data is to determine $f_F(D)$ unambiguously. A second distribution function can be defined, $f_P(l)$, which specifies the fraction of actin monomers which are part of polymers of length $\ell \pm \mathrm{d}\ell$. The fluorescence recovery is then expressed as

$$i_F(t) = \int_{l_0}^{\infty} i_F[t, D(\ell)]\, f_P(\ell)\, \mathrm{d}\ell, \tag{2}$$

and the two distribution functions are related by the differential equation

$$-f_P(\ell) = f_F(D)\frac{dD}{d\ell}. \tag{3}$$

Determination of filament size by electron microscopy shows that mean lengths can exceed 1 μm, with some filaments >10 μm (10).

In solutions where the polymerization of actin can proceed, sequential measurement of FPR should show a change in fluorescence mobility distribution away from the mobility of the actin monomer to that of the long filament. Measurement of that time-dependent process is the focus of this report.

THEORY AND DESIGN OF FPR APPARATUS

The most compact and commonly employed probe beam for FPR measurement is a Gaussian beam produced by a laser and brought to a focus at the sample (21). For these experiments we chose to use a focal Airy pattern, because the node diameter is easily measured through the microscope. This dimension enters into the computation of the diffusion coefficient in nearly the same way as r_0, the width parameter of a Gaussian beam. The disadvantage of using the Airy pattern is that the mathematical form of the resulting fluorescence recovery cannot be expressed simply, which makes the inversion of FPR data a longer procedure.

The intensity field in the plane of the sample is described by

$$I_A(r) = I_A(0)\, 4\, J_1^2(br)/b^2r^2 \tag{4}$$

where J_1 is a first-order Bessel function. $I_A(r)$ has a bright central spot surrounded by concentric rings of decreasing intensity. This pattern is less localized than a Gaussian beam of equal power; the intensity envelope decays asymptotically as r^{-3}.

The Airy pattern is produced by bringing to a focus the part of a plane wave that has passed an adjacent circular aperture. The width parameter (b) is defined by the wavelength and f-number of the optical system, and defines the pattern "size":

$$\pi a/\lambda f = b = 2j_n/d_n = 7.66/d_1. \tag{5}$$

Here, a is aperture diameter, f is local length, j_n is the nth root of $J_1(z)$, and d_n is the diameter of the nth node of the Airy pattern. A suitably defined depth-of-field (23) is given by

$$\delta = 0.25\,\lambda f^2/a^2 = 0.042\, d_1^2/\lambda. \tag{6}$$

For FPR measurement in bulk solution, the depth-of-field is an important consideration, since cylindrical symmetry of the radiation field through the sample greatly simplifies the theory of the fluorescence recovery.

The initial label concentration profile bleached at $t = 0$ in an FPR experiment is proportional to $\exp(-KI_A(r))$ under the proper conditions. If the label concentration gradient dissipates due to diffusion only, the fluorescence recovery is specified by

$$F(t) = \alpha_F \int I_m(r) \int c_0 e^{-KI_A(r')} g(r, r', t)\, ds'ds, \tag{7}$$

where $g(r, r', t)$ is Green's function for free diffusion (in cylindrical coordinates), and $I_m(r)$ is the monitoring intensity field, which in our system is the same pattern used for bleaching, highly attenuated.

By expanding the exponentiated illumination field as a power series, $F(t)$ can be computed accurately. The first-order term in this series approximates the fluorescence recovery in the low bleaching limit:

$$i_F(t)/i_F(0) = 7.054 \int_0^1 [\cos^{-1}u - u(1 - u^2)^{1/2}]^2 e^{-4b^2Dtu^2} u\,du. \quad (8)$$

This integral can be completed and yields a complex series of exponential and Bessel functions, with argument $2b^2Dt$. For computational purposes, the above form is more convenient. Under typical experimental conditions, where the fluorescence of the sample is initially reduced 10–25% by bleaching, the second-order integral is also required for accurate data analysis. The relation between the FPR half-life ($t_{1/2}$) and the diffusion coefficient of the labeled particle is:

$$D = \gamma\, d_1^2/t_{1/2} \quad (9)$$

where d_1 is the Airy disc diameter and γ is a numerical coefficient that is a function of the initial degree of bleaching. The value of γ varies from 0.0278, in the limit $K = 0$, to >0.029 when $K > 0.5$. The latter value of γ corresponds to an initial bleached fraction of 20%.

As in most other FPR systems, our apparatus consists of an illuminator, microscope, and photometer. A flat glass capillary tube, with an internal space 50–100 μm deep, is filled with the test solution and fixed to the stage of the microscope. The short optical path is important because the scattering cross section (turbidity) of a test solution can be significant, especially when filaments or aggregates are present. It is also important that the absorbance of the sample be low enough so that dI/dx, the amount of absorbed light per unit distance in the sample, is nearly constant through the sample. For a light source we use an argon ion laser operating at 488 nm. The linearly polarized beam passes through a mica quarter-wave plate, adjusted to produce circular polarization. This prevents the possibility of net anisotropic bleaching of immobilized fluorophores, which could cause a fluorescence recovery by rotational diffusion in addition to translation.[1] An intense point source of light is produced by focusing the laser beam onto a pinhole filter. The condenser illuminates a small part of the test solution by imaging the point source at finite aperture in the plane of the sample. The resulting intensity distribution, which has a depth-of-field greater than the sample thickness, is an Airy pattern. The size of the pattern varies inversely with the aperture and is typically set so that d_1, the Airy disc diameter, is ~100 μm. The illuminated volume of test solution is thus ~1 nl.

Brief, intense illumination for bleaching is produced by the operation of a solenoid-driven filter in the path of the laser beam. This filter is corrected to minimize beam steering, and has an absorbance of ~4.8. Without attentuation by the filter, the intensity at the center of the Airy pattern is typically 250 W/cm^2. Depending upon the particular labeled species, an exposure of 30–200 ms is required to produce an optimal amount of bleaching, typically 20–30% of the total emission.

A microscope objective lens collimates the fluorescence emitted by the sample. This is followed by a barrier filter (OG515, Schott Optical Glass, Duryea, Pa.) selected to pass the emission of fluorescein (>515 nm) and strongly absorb the laser radiation (488 nm). Because the barrier filter also fluoresces when excited at 488 nm, a simple spatial filter follows, which passes the collimated sample fluorescence with high efficiency, but which transmits only a small fraction of the isotropically radiated filter fluorescence. The detector is a photomultiplier tube protected by a fast electromechanical shutter, which opens a few milliseconds after the end of a bleaching pulse. The output of the detector is amplified and recorded on a strip chart. An independent photodiode circuit marks the bleaching event on the chart record.

Two types of FPR control experiments were performed. To determine that signal recoveries were not due to transients in the optical path or in the electronics, the barrier filter was replaced by a neutral attenuator, and a scattering, nonfluorescent target was used as a test sample. Operation of the bleaching cycle caused no transient in the amount of scattered light reaching the photomultiplier. With the barrier filter in place, only a small, stationary background signal was present. To determine that the observed

[1]Dr. Barton A. Smith, personal communication.

fluorescence recoveries and our theory of measurement were consistent, solutions of labeled macromolecules of known mobility were used as test samples (ovalbumin and bovine serum albumin [BSA] labeled with fluorescein isothiocyanate [FITC]). Free fluorescein dye (332 mol wt) was also used as a high-mobility test particle.

A thermal transient is produced in the sample during bleaching, owing to absorbed radiation that is not reemitted as fluorescence. An analysis of this problem was presented by Axelrod (24) for a two-dimensional absorber in a three-dimensional bath, with the result that an insignificant, bounded temperature increase occurred. For a bulk absorber, solution of Fourier's equation with boundary conditions imposed by intensity distribution and duration, thermal conductivity, absorbance, and heat capacity, yields $\Delta T = +0.5°C$ as the maximum temperature increase at the center of the bleached volume in these experiments. Unlike the two-dimensional system, ΔT diverges logarithmically, limited by the duration of bleaching. This small local temperature rise dissipates rapidly after bleaching, so that the fluorescence recovery occurs at the temperature of the bulk phase.

The kinetics of the irreversible photochemical reaction that bleaches the fluorescent label specifies the relation between illumination pattern and bleached profile in the sample, and must be known in order to analyze FPR data accurately. (Scanning or imaging methods obviate this problem [25, 26]) In particular, if the bleaching reaction requires absorption of n photons, the local bleaching rate constant will be proportional to $I(r)^n$, where $I(r)$ is the local intensity. The value of n can be determined if a simultaneous measurement of fluorescence and bleaching rate is made at two different excitation intensities, under conditions where fluorescence recovery due to diffusion or other transport processes is not possible. Using solutions of FITC-labeled dextran (FD20, FD150, Sigma Chemical Co., St. Louis, Mo.) and FITC-labeled ovalbumin, we determined that for fluorescein, $n = 1$ (1.08 ± 0.12 RMSE), and that the photobleaching reaction requires oxygen. Dissolved oxygen is normally present in aqueous solution at an equilibrium concentration of roughly 0.2 mM (27), and is therefore always present in excess of fluorescent dye. The local bleaching rate constant is therefore proportional to the first power of $I(r)$, and the local bleaching rate in an FPR experiment is thus an exponential function of $I(r)$. A first-order bleaching process such as this was assumed by Axelrod et al. (21) in their first presentation of the FPR method.

Preparation of Experimental Materials

Rabbit muscle actin used in these experiments was prepared by the method of Spudich and Watt (28), and purified by cycles of polymerization and depolymerization. Depolymerization was effected by dialyzing a suspension of F-actin against a bath of low ionic strength buffer (buffer A: 2 mM Tris (pH 8), 0.2 mM $CaCl_2$, 1.0 mM ATP, 0.5 mM dithiothreitol [DTT]). Dialyses were performed in closed bottles at 4°C. The resulting solution was clarified by centrifugation at 10^5 g for 30 min at 4°C to pellet aggregates and large particles. Salt (KCl to 100 mM) and magnesium ($MgCl_2$ to 2 mM) were added to the clarified supernatant, which was allowed to stand for at least 1 h at room temperature. The resulting solution of polymerized actin was then sedimented at 10^5 g for 2 h at 15°C, resulting in an F-actin pellet. In order to produce solutions of low Mg^{+2} content, repolymerization was often initiated by addition of salt alone, without any noticeable loss of recovered F-actin. Sodium azide was used to suppress bacterial growth in our protein solutions, but because 0.02% NaN_3 increases the ionic strength of a solution by 3 mM, it was often not added to final dialysis buffers. In addition, we observed that both azide and DTT reduced the efficiency of the photobleaching reaction.

For some measurements, it was important that the test solutions be free of dissolved oxygen. Buffers and other protein-free solutions were degassed under vacuum and flushed with nitrogen several times. Protein solutions were deoxygenated by dialysis in a bath continuously flushed with water-saturated nitrogen. Transfers of deoxygenated solutions were made in a nitrogen-filled glove bag. Glass capillary tubes containing FPR samples were routinely sealed with Vaseline (Chesebrough-Ponds, Greenwich, Conn.), and it was noted that with deoxygenated solutions, reoxygenation occurred at the sealed ends of the capillaries, probably because of oxygen dissolved in the grease seal.

Using the procedure of Taylor and Wang (13), we reacted filamentous actin with the sulfhydryl-specific probe, 5-iodoacetamido fluorescein (5-IAF, Molecular Probes Inc., Plano, Tex.). This produces

actin labeled mainly at cysteine 373. The AF-actin was purified by chromatography and by cycles of depolymerization, sedimentation, repolymerization, and pelleting. Wang and Taylor (29) have used AF-actin in microinjection experiments and have demonstrated its biological activity by comparing its cytoplasmic fluorescence distribution to that of an "inert" control protein such as FTC-ovalbumin.

Fluorescein-labeled actin was also produced by reaction of F-actin with the amino-specific probe, fluorescein isothiocyanate. FTC-actin so produced is less well characterized than AF-actin, but polymerizes and depolymerizes under typical conditions. Since the primary sequence of the rabbit muscle actin used (30) includes many amino-bearing residues, it is likely that FTC-actin is a mixture of populations differing in probe location. The amount of FITC used was adjusted so that the degree of labeling was close to that obtained with IAF, a dye-to-protein ratio of 0.8–1.0.

Labeled actin was stored on ice either as a low ionic strength solution or as a wet pellet. Storage as a pellet was found to be preferable, since a noticeable loss of polymerizability occurred in solutions stored more than a few days, even after further dialysis.

The flat glass capillary tubes used for FPR measurement (Vitro Dynamics Inc., Rockaway, N.J.) were washed and drained by centrifugation. For initial washes, a dilute solution of BSA in phosphate buffer was used, followed by several washes in buffer A. The capillary tubes were stored at 4°C. The purpose of this procedure was to produce a surface which would not have any high-affinity binding sites for protein, especially in low ionic strength solution. Capillary tubes so treated do not fill spontaneously by surface tension, but are easily filled by applying a slight suction to one end.

Test solutions stored on ice were loaded into capillary tubes at room temperature, sealed, and clamped to the stage of the FPR microscope. Any additions made to the actin stock solutions were made at 0°C immediately before loading. To produce conditions under which polymerization will proceed, salt (KCl up to 100 mM) or magnesium ($MgCl_2$, 1–5 mM) was added to the cold actin stock and the solution quickly loaded. The small dimensions of the capillary tube allow thermal equilibration to occur within a few seconds, so that for time-dependent assays of polymerization, $t = 0$ was well defined. As no large temperature excursions occurred while the sample was in the microscope, all measurements were made at ambient temperature. Measurements of photobleaching recovery were made at intervals of several minutes, each time bleaching at a different location in the sample. This prevented the slowly dissipating components of previous photobleaching cycles from interfering with subsequent measurements. Sample mixing, loading, mounting, and alignment required about 4 min before the first FPR measurement was made.

RESULTS

FPR control experiments gave diffusion coefficients consistent with recovery due to translational diffusion. For fluorescein in aqueous buffer, we measured $D_{20,w}$ (the diffusion coefficient corrected to the viscosity of water at 20°C) = $(2.5 \pm 1.0) \times 10^{-6}$cm^2/s. As an upper limit for the mobility of fluorescein, an equivalent-sphere frictional coefficient can be computed from the molecular dimensions, yielding $D_{max} = 5 \times 10^{-6}$cm^2/s. For FTC-ovalbumin (45,000 mol wt), we found $D_{20,w}$ to be $(6.63 \pm 0.46) \times 10^{-7}$ cm^2/s, and for FTC-BSA (65,000 mol wt), we found $D_{20,w}$ to be $(5.54 \pm 0.34) \times 10^{-7}$ cm^2/s. The BSA and ovalbumin test samples had a protein concentration of ~1 mg/ml, and were equilibrated with 10 mM Tris (pH 7.4) by dialysis. Both of these coefficients are slightly lower than the generally accepted values of 7.76×10^{-7} and 6.14×10^{-7} cm^2/s, respectively (31, 32). From each FPR record, the diffusion coefficient was determined by a graphical procedure that introduces a systematic negative error. The reported coefficients are averaged values, having the variance indicated. The major sources of instrumental error are also systematic and negative; the finite width of the sample capillary, residual beam steering (33), mechanical transients, and the finite duration of the bleaching period all act to reduce the speed of fluorescence recovery.

Control experiments for the polymerization of actin were performed with solutions of IAF-actin to which no salt or Mg^{+2} had been added. Actin is stable as a low molecular weight form in buffer A. After photobleaching, fluorescence returned to its initial level, which indicates that there was an insignificant amount of filamentous actin present. On the assumption that there is not a broad distribution of molecular sizes in this depolymerized sample, a mean diffusion coefficient can be determined from the half-life of the fluorescence recovery. Diffusion coefficients ($D_{20,w}$) ranged from 6.1×10^{-7} cm^2/s for freshly prepared and depolymerized AF-actin, to 4.9×10^{-7} cm^2/s for FTC-actin which has been dialyzed for several days in buffer A. This range includes the value determined for G-ADP-actin by Mihashi (34), by means of a sedimentation boundary method, 5.28×10^{-7} cm^2/s.

When the ionic strength of buffer A was increased by addition of KCl to 100 mM, the polymerization of AF-actin occured within 30 min at 25°C when the total actin concentration was 0.5–1.0 mg/ml. The FPR traces obtained (Fig. 1) show two major features: a recovery that occurs at a rate typical of actin in low salt buffer, and a fraction for which there is no fluorescence recovery. Our interpretation of the FPR trace is that polymerization, once initiated, proceeds rapidly. This creates a bimodal molecular size distribution of long

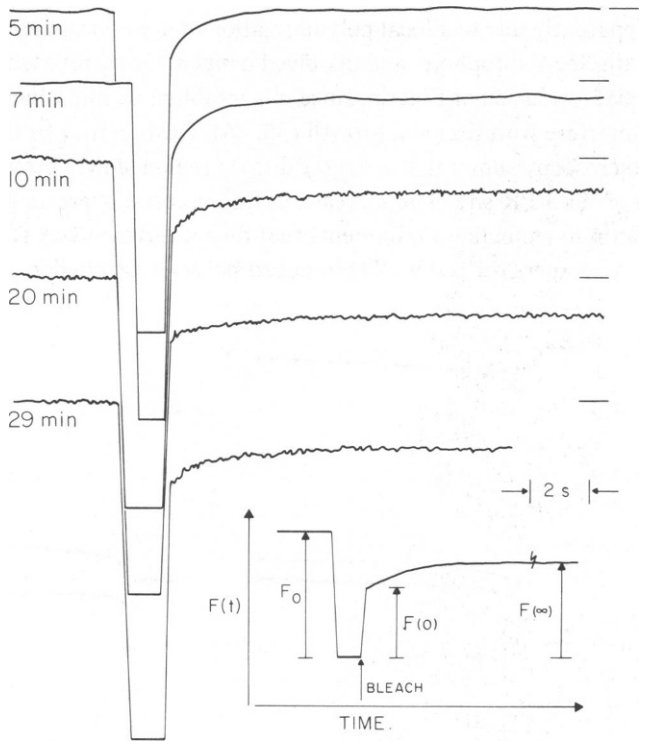

FIGURE 1 Fluorescence recovery of AF-actin in high-salt buffer. Filamentous AF-actin was depolymerized by dialysis in buffer A (1mM ATP, 0.5mM DTT, 0.2mM $CaCl_2$, 2mM Tris, pH 8.0, at 25°C) At t = 0, concentrated KCl was added to 100 mM. FPR measurements were made every few minutes, as indicated. For each FPR record, $F(0)$ was determined by extrapolation of $F(t)$ to the time at which bleacing occurred. [Actin] ≈ 0.5 mg/ml.

filaments with essentially zero mobility, and monomers or low polymers which are not growing rapidly. If all labeled species in solution bleach with the same rate constant, and have the same overall fluorescence quantum efficiency, the ratio $[F_0 - F(\infty)]/[F_0 - F(0)]$, as indicated in Fig. 1, is a direct measure of the fraction of label that is immobile (f_{IM}) on the time scale of the measurement. The observed fluorescence emission of both AF-actin and FTC-actin was slightly reduced as the ionic strength of buffer A was increased or when Mg^{+2} was added, and markedly reduced when both were added to the buffer (Fig. 2). These changes seem to occur immediately upon addition of salt or Mg^{+2} to buffer A, and are much less dependent upon the degree of polymerization of the actin. In addition, both unpolymerized and filamentous actin bleach to nearly the same extent in response to the same exposure, so that the above ratio is a good measure of f_{IM}. The graph of $f_{IM}(t)$ for AF-actin in high-salt buffer (Fig. 3) shows that several minutes elapse before low-mobility fluorescence is detectable and that a steady state is reached within 30 min. Depletion of buffer ATP after several hours will cause this steady state to decay to an equilibrium state.

During the period in which $f_{IM}(t)$ increases most rapidly, photobleaching a solution of AF-actin gives rise to a fluorescence recovery followed by a slow increase in the fluorescence emission of the sample well beyond the initial level. The rate of increase is a function of exposure of the sample, multiple exposures at one location increasing the rate proportionally (Fig. 4). This is apparently due to a local polymerization of actin initiated by a photochemical event involving actin, the fluorophore, and dissolved oxygen. Once initiated, the process seems to proceed by normal formation of F-actin, since it is inhibited by micromolar Cytochalasin B, a toxin known to interfere with filament growth (35, 36). Examination of the sample capillary by fluorescence microscopy shows that a bright diffuse region slowly grows radially outward from the location of the FPR site. The increase in fluorescence is presumed to be due to the incorporation of actin monomers into filaments that do not diffuse away from the illuminated volume as fast as monomers diffuse in. The induced polymerization does not occur in buffer

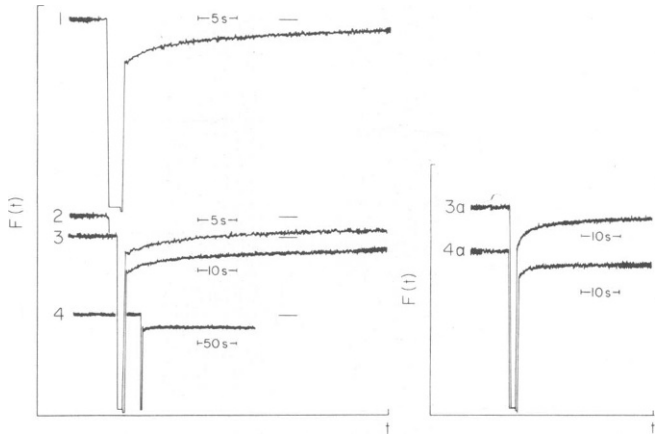

FIGURE 2 Fluorescence recovery in solutions of FTC-actin. Trace 1: FTC-actin in buffer A. Traces 2 and 3: 25 min after addition of salt or $MgCl_2$, respectively. Trace 4: 6 min after addition of salt and $MgCl_2$. Traces 3*a* and 4*a*: fluorescence recovery of samples 3 and 4 after 18 h at room temperature. All except trace 1 are drawn with the same gain and base line to show the effect of salt, Mg^{+2}, and ATP on the overall fluorescence quantum efficiency.

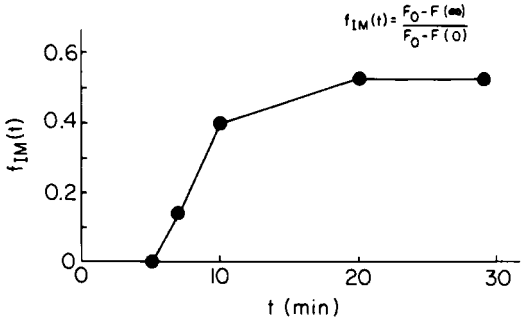

FIGURE 3 Appearance of low-mobility fluorescence in a solution of polymerizing AF-actin. Conditions are those described in Fig. 1.

that has been carefully deoxygenated (and in which photobleaching of fluorescein does not occur).

To determine whether induced polymerization of actin is a specific problem with AF-actin, or a general problem of dye sensitization, we prepared and used FTC-actin in a similar experiment. Since we have observed neither photoinduced polymerization under polymerizing conditions nor photoinduced depolymerization of gelled FTC-actin, we infer that the location of the fluorophore on the actin monomer determines its reactivity.

Fig. 2 shows fluorescence recovery in solutions of FTC-actin. The data have been treated as described, with a mean diffusion coefficient computed from the half-life of the mobile fraction of fluorescence. For actin in buffer A (trace 1), $D_{20,w} = 4.9 \times 10^{-7}$ cm^2/s when corrected for systematic error, which is slightly lower than that determined by Mihashi for G-ADP-actin. In the presence of salt or Mg^{+2}, the recovery half-life increased by ~40% after 25–30 min at 25°C (traces 2 and 3), which indicates that the mean particle size increased under these conditions. In the sample containing Mg^{+2}, the fluorescence recovery was incomplete (f_{IM} = 21%) several minutes after bleaching, which indicates the presence of immobile fluorophore. Trace 4 is characteristic of actin activated by both salt and Mg^{+2}; typically, polymerization was complete by the time the first FPR measurement could be made (about 4 min after addition of salt and Mg^{+2}), and essentially all fluorescent label was immobile. Traces 2, 3, and 4 were recorded with the same gain and base line to show the effects of salt and Mg^{+2} upon

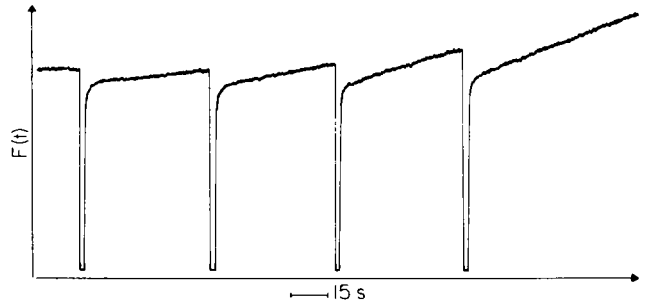

FIGURE 4 Multiple-bleach sequence showing induced polymerization of AF-actin in high-salt buffer.

the overall fluorescence quantum efficiency. A similar effect was observed with AF-actin. The polymerization of FTC-actin induced by salt or Mg^{+2} was sluggish compared with AF-actin under the same conditions.

Traces 3*a* and 4*a* were obtained after storage of samples 3 and 4 for 18 h at room temperature. Both were recorded at the same gain as 2, 3, and 4, and show an immobile fraction that is smaller in each case than before storage, and a mean diffusion coefficient which is approximately that expected for the actin monomer if it is a compact and nearly spherical particle. A hypothesis to explain the appearance of a rapidly diffusing component in these solutions is that buffer ATP is gradually depleted by the actin ATPase function under polymerizing conditions, and an ATP-depleted equilibrium state is attained where monomeric FTC-actin is present in greater amounts than when ATP is present.

DISCUSSION

Actin is a highly conserved protein that interacts specifically with other actin molecules, protein elements of the contractile apparatus and cytoskeleton (28, 37, 18, 38, 39, 40, 10, 41), regulator proteins from muscle and nonmuscle tissues (42–46), free nucleotides, divalent metal ions, and the poisonous phalloidins and cytochalasins. Fluorescence photobleaching recovery affords a way to investigate many of these interactions without subjecting the soluble system to a separation procedure or to mechanical stress. Using FPR to investigate solutions of fluorescein-labeled actin, we have been able to monitor its state of polymerization under equilibrium, stationary, and time-dependent conditions.

Our actin FPR data show two major features, which allow a simple analysis: a fraction of the recovery occurs with a half-life characteristic of small aggregates of actin monomers, and the remainder of the label is immobile on the time scale of the experiment. Our conclusion is that filament growth is rapid but that initiation events occur relatively slowly. This is in accord with the results of other investigators (47, 48). Using a light-scattering technique, Wegner (17) generated a graph of the time-dependent concentration of monomeric actin under polymerizing conditions (high salt); this graph and $f_{IM}(t)$ are complementary functions, and are in accord with our results.

The data regarding the mobility of G-actin do not form a consistent picture. Examination of negatively-stained filaments by electron microscopy (9) shows the actin subunits to be compact, nearly spherical particles with a maximum diameter of 55 Å. These would have a hard-sphere diffusion coefficient near 8×10^{-7} cm^2/s in the monomeric state. The diffusion coefficient obtained for AF-actin is therefore low for a globular protein of 4.2×10^4 mol wt (49). Several hypotheses could explain this difference. If buffer A did not cause complete depolymerization of F-actin, a low diffusion coefficient would be determined. But this would fail to explain why the rate of appearance of immobile fluorescence is not immediately maximal upon addition of salt (Fig. 3). A second possibility is that G-actin is extended or noncompact in low-salt buffer. A third factor is that measurements involving native G-actin are necessarily made with a low ionic strength buffer to suppress assembly. Thus the electrostatic interaction between the protein and its counterions reduces the tracer diffusion coefficient. We are performing further experiments to determine the magnitude of this effect.

Under constant conditions a solution of actin will attain a steady state in terms of the rate of hydrolysis of ATP, and, presumably, in terms of the distribution of filament lengths. In the polymerization process, the number of reactive sites (monomers plus filament ends) decreases as the amount of filamentous material increases. At some point the total rate at which monomers add to filament ends will be balanced by the rate of dissociation from filament ends. If some early step of filament formation is positively cooperative, a critical concentration will be defined; $[\text{G-actin}]_c = k_d/k_a$. In a solution where the total concentration of actin is less than critical, no filaments form. When the total amount of actin exceeds the critical concentration, the excess will be filamentous (47). A more detailed model of actin polymerization would specify the highly asymmetric nature of the polymerization under nonequilibrium conditions; the rate constant for addition at one end of the polar filament would be very large, with depolymerization occurring mainly at the other end. This is the head-to-tail model of actin filament structure proposed by Wegner (17), which also explains the results of several recent experiments testing the effects of cytochalasins on filament formation (10, 35, 50–52). The rate constants k_a and k_d are thus functions of the system composition, particularly the amount of ATP and ADP present. In an FPR experiment, the mobile fluorescence will be due to the critical concentration of G-actin and oligomers. When steady-state conditions are attained in a polymerization buffer system, most of the filamentous actin has a very low mobility, and the mobile fluorescence becomes a measure of the critical concentration. From our data (Fig. 2), the mobile fraction of FTC-actin in the presence of ATP, salt, and Mg^{+2} (trace 4), is <15% of the total bleached fraction. Since the concentration of actin in this solution was ~1 mg/ml, the critical concentration under these polymerizing conditions is <3.5 μM.

Because of the large number of specific interactions involving the actin monomer, it is very possible that chemical modification of actin at any location will affect some aspect of its biological activity or biochemical function. AF-actin is incorporated into cytoplasmic structures, and can be polymerized or depolymerized under conditions typical for unlabeled actin, but undergoes a photochemical reaction which changes its polymerizability, which makes it difficult to use as a tracer particle for FPR. FTC-actin also polymerizes and depolymerizes under standard conditions, but does so more slowly than AF-actin.

Photochemically induced polymerization of AF-actin complicated the results of these experiments. We have not determined whether this photochemical event causes the formation of F-actin "seeds" that initiate new filaments, or whether existing filaments are cleaved, creating new growing ends. Since induced polymerization is not detectable until some spontaneous polymerization has occurred, the latter hypothesis is supported. In solutions of filamentous AF-actin, photobleaching produces, in addition to an immediate decrease in emission, a slow loss that we attribute to the local breakage of filaments into smaller fragments of higher mobility (data not shown). Early viscometric studies by Martonosi and Gouvea (53) demonstrated that the photodynamic action of the dye methylene blue, now thought to be mediated by singlet oxygen (54), caused F-actin to depolymerize and deactivated G-actin. More recently, measurements of fluorescence resonance energy transfer have demonstrated that the labeling site Cys373 has at least one aromatic amino acid residue as a near neighbor (55). A bifunctional cross-linking reagent also has been used to show that Cys373 is located near one of the domains between actin monomers in a filament (56). Our

hypothesis is that when fluorescein is coupled to actin at Cys373, it appears to be in a position where photooxidation of a residue on the actin monomer, or on one of its neighbors in a filament, can occur with measurable efficiency. If this causes a complete break in the double-stranded filament, two new ends are created, at least one of which is capable of growth by addition of monomers. Moving the fluorophore to another location on the macromolecule is only one approach to eliminating this as an artefact in FPR measurement. Fluorescent probes other than fluorescein, not all of which activate oxygen (57), could be used in similar experiments. It is an advantage of this tracer method that a wide variety of labels are available that differ in their spectral and chemical properties. Possibly, the photosensitivity of certain labeled actins can be exploited to inactivate some subcellular structures in vivo (29). This may, for instance, provide a way to assess the role of actin in different parts of the mitotic spindle.

One of the purposes of this research is to provide a basis for the interpretation of future experiments in which the local mobility of labeled actin that has been microinjected into a living cell is determined by FPR. Such an experiment would be of great interest in the study of motile cells or of stationary cells with changing cytoplasmic structure. Another extension of these experiments is the study of the binding of other macromolecules to actin. Such filaments have a very low mobility, the apparent diffusion coefficient of a labeled protein that binds to actin will be lowered in the fast-exchange limit, or, in the slow-exchange limit, the fluorescence recovery will be split into an immobile fraction and a normally diffusing fraction. We believe that FPR will prove to be a valuable technique for the study of cytoplasmic motility, and other problems involving supramolecular assembly.

The authors are grateful to Mrs. Mara Aistars for expert technical assistance, and to Catherine Becker Lanni for manuscript preparation.

This work was supported by grant PCM-8010924 from the National Science Foundation.

Received for publication 24 November 1980 and in revised form 9 February 1981.

REFERENCES

1. Straub, F. B., and G. Feuer. 1950. Adenosinetriphosphate, the functional group of actin. *Biochim. Biophys. Acta.* 4:455–470.
2. Asakura, S., and F. Oosawa. 1960. Dephosphorylation of adenosine triphosphate in actin solutions at low concentrations of magnesium. *Arch. Biochem. Biophys.* 87:273–280.
3. Kasai, M., S. Asakura, and F. Oosawa. 1962. The G-F equilibrium in actin solutions under various conditions. *Biochim. Biophys. Acta.* 57:13–21.
4. Kasai, M., S. Asakura, and F. Oosawa. 1962. The cooperative nature of G-F transformation in actin. *Biochim. Biophys. Acta.* 57:22–31.
5. Asakura, S., M. Taniguchi, and F. Oosawa. 1963. Mechano-chemical behavior of F-actin. *J. Mol. Biol.* 7:55–69.
6. Fujime, S., and S. Ishiwata. 1971. Dynamic study of F-actin by quasi-elastic scattering of laser light. *J. Mol. Biol.* 62:251–265.
7. Newman, J., and F. D. Carlson. 1980. Dynamic light scattering evidence for the flexibility of native muscle thin filaments. *Biophys. J.* 29:37–48.
8. Kawamura, M., and K. Maruyama. 1969. Particle length of actomyosin measured by electron microscopy. *J. Biochem. (Tokyo).* 66:619–626.
9. Moore, P. B., H. E. Huxley, and D. J. DeRosier. 1970. Three-dimensional reconstruction of F-actin, thin filaments, and decorated thin filaments. *J. Mol. Biol.* 50:279–295.

10. Hartwig, J. H., and T. P. Stossel. 1979. Cytochalasin B and the structure of actin gels. *J. Mol. Biol.* 134:539–553.
11. Cheung, H. C., R. Cooke, and L. Smith. 1971. The G-actin → F-actin transformation as studied by the fluorescence of bound dansyl-cysteine. *Arch. Biochem. Biophys.* 142:333–339.
12. Kawasaki, Y., K. Mihashi, H. Tanaka, and H. Ohnuma. 1976. Fluorescence study of N-(3-pyrene)-maleimide conjugated to rabbit skeletal F-actin and plasmodium actin polymers. *Biochim. Biophys. Acta.* 446:166–178.
13. Taylor, D. L., and Y.-L. Wang. 1978. Molecular cytochemistry: incorporation of fluorescently labeled actin into living cells. *Proc. Natl. Acad. Sci. U.S.A.* 75:857–861.
14. Wulf, E., A. Deboben, F. A. Bautz, H. Faulstich, and Th. Wieland. 1979. Fluorescent phallotoxin, a tool for the visualization of cellular actin. *Proc. Natl. Acad. Sci. U.S.A.* 76:4498–4502.
15. Thomas, D. D., J. C. Seidel, and J. Gergely. 1979. Rotational dynamics of spin-labeled F-actin in the submillisecond time range. *J. Mol. Biol.* 132:257–273.
16. Harwell, O. D., M. L. Sweeney, and F. H. Kirkpatrick. 1980. Conformational changes of actin during formation of filaments and paracrystals and upon interaction with DNase I, Cytochalasin B, and phalloidin. *J. Biol. Chem.* 255:1210–1220.
17. Wegner, A. 1976. Head-to-tail polymerization of actin. *J. Mol. Biol.* 108:139–150.
18. Pollard, T. D. 1976. The role of actin in the temperature-dependent gelation and contraction of extracts of acanthamoeba. *J. Cell Biol.* 68:579–601.
19. Peters, R., J. Peters, K. H. Tews, and W. Bahr. 1974. A microfluorimetric study of translational diffusion in erythrocyte membranes. *Biochim. Biophys. Acta.* 367:282–294.
20. Jacobson, K., E. Wu, and G. Poste. 1976. Measurement of the translational mobility of concanavalin A in glycerol-saline solutions, and on the cell surface by fluorescence recovery after photobleaching. *Biochim. Biophys. Acta.* 433:215–222.
21. Axelrod, D., D. E. Koppel, J. Schlessinger, E. Elson, and W. W. Webb. 1976. Mobility measurement by analysis of fluorescence photobleaching recovery kinetics. *Biophys. J.* 16:1055–1069.
22. Barisas, B. G., and M. D. Leuther. 1979. Fluorescence photobleaching recovery measurement of protein absolute diffusion coefficients. *Biophys. Chem.* 10:221–229.
23. M. Born, and E. Wolf. 1964. Principles of Optics, 2nd Ed. The MacMillan Co., New York.
24. Axelrod, D. 1977. Cell surface heating during fluorescence photobleaching recovery experiments. *Biophys. J.* 18:129–131.
25. Koppel, D. E. 1979. Fluorescence redistribution after photobleaching. *Biophys. J.* 28:281–292.
26. Smith, B. A., and H. M. McConnell. 1978. Determination of molecular motion in membranes using periodic pattern photobleaching. *Proc. Natl. Acad. Sci. U.S.A.* 75:2759–2763.
27. G. W. Castellan. 1964. Physical Chemistry. Addison-Wesley Publishing Co. Inc., Reading, Mass.
28. Spudich, J. A., and S. Watt. 1971. The regulation of rabbit skeletal muscle contraction. *J. Biol. Chem.* 246:4866–4871.
29. Wang, Y.-L., and D. L. Taylor. 1979. Distribution of fluorescently labeled actin in living sea urchin eggs during early development. *J. Cell Biol.* 81:672–679.
30. Collins, J. H., M. Elzinga, and N. Jackman. 1975. The primary structure of actin from rabbit skeletal muscle. *J. Biol. Chem.* 250:5915–5920.
31. Lamm, O., and A. Polson. 1936. The determination of diffusion constants of proteins by a refractometric method. *Biochem. J.* 30:528–541.
32. Creeth, J. M. 1952. The use of the Gouy diffusiometer with dilute protein solutions: an assessment of the accuracy of the method. *Biochem. J.* 51:10–17.
33. Barisas, B. G. 1980. Criticality of beam alignment in fluorescence photobleaching recovery experiments. *Biophys. J.* 29:545–548.
34. Mihashi, K. 1964. Molecular characteristics of G-ADP-actin. *Arch. Biochem. Biophys.* 107:441–448.
35. Brown, S. S., and J. A. Spudich. 1979. Cytochalasin inhibits the rate of elongation of actin filament fragments. *J. Cell Biol.* 83:657–662.
36. Chang Lin, D., K. Dugan Tobin, M. Grumet, and S. Lin. 1980. Cytochalasins inhibit nuclei-induced actin polymerization by blocking filament elongation. *J. Cell Biol.* 84:455–460.
37. Pollard, T. D., and R. R. Weihing. 1974. Actin and myosin and cell movement. *Crit. Rev. Biochem.* 2:1–65.
38. Clarke, M., and J. A. Spudich. 1977. Nonmuscle contractile proteins: the role of actin and myosin in cell motility and shape determination. *Annu. Rev. Biochem.* 46:797–822.
39. Zeece, M. G., R. M. Robson, and P. J. Bechtel. 1979. Interaction of α-actinin, filamin, and tropomyosin with F-actin. *Biochim. Biophys. Acta.* 581:365–370.
40. Condeelis, J. S., and D. L. Taylor. 1977. The contractile basis of amoeboid movement. V. The control of gelation, solation, and contraction in extracts from dictyostelium discoideum. *J. Cell Biol.* 74:901–927.

41. Hellewell, S. B., and D. L. Taylor. 1979. The contractile basis of amoeboid movement. VI. The solation-contraction coupling hypothesis. *J. Cell Biol.* 83:633–648.
42. Wang, K., and S. J. Singer. 1977. Interaction of filamin with F-actin in solution. *Proc. Natl. Acad. Sci. U.S.A.* 74:2021–2025.
43. Schloss, J. A., and R. D. Goldman. 1979. Isolation of a high molecular weight actin-binding protein from baby hamster kidney cells. *Proc. Natl. Acad. Sci. U.S.A.* 76:4484–4488.
44. Yin, H. L., and T. P. Stossel. 1979. Control of cytoplasmic actin gel-sol transformation by gelsolin, a calcium-dependent regulatory protein. *Nature (Lond.).* 281:583–586.
45. Mimura, N., and A. Asano. 1979. Ca^{+2}-sensitive gelation of actin filaments by a new protein factor. *Nature (Lond.).* 282:44–48.
46. Taylor, D. L., and J. S. Condeelis. 1979. Cytoplasmic structure and contractility in amoeboid cells. *Int. Rev. Cytol.* 56:57–144.
47. Oosawa, F., and M. Kasai. 1971. Actin. *In* Biological Macromolecules, Vol. 5. S. N. Timasheff and G. D. Fasman, Eds., Marcel Dekker, Inc., New York. 261–322.
48. Gordon, D. J., Y.-Z. Yang, and E. D. Korn. 1976. Polymerization of acanthamoeba actin. *J. Biol. Chem.* 251:7474–7479.
49. Elzinga, M., J. H. Collins, W. M. Kuehl, and R. S. Adelstein. 1973. Complete amino-acid sequence of actin of rabbit skeletal muscle. *Proc. Natl. Acad. Sci. U.S.A.* 70:2687–2691.
50. MacLean-Fletcher, S., and T. D. Pollard. 1980. Mechanism of action of cytochalasin B on actin. *Cell.* 20:329–341.
51. Flanagan, M., and S. Lin. 1980. Cytochalasins block actin filament elongation by binding to high-affinity sites associated with F-actin. *J. Biol. Chem.* 255:835–838.
52. Brenner, S., and E. D. Korn. 1979. Substoichiometric concentrations of cytochalasin D inhibition actin polymerization. *J. Biol. Chem.* 254:9982–9985.
53. Martonosi, A., and M. A. Gouvea. 1960. Studies on actin. V. Chemical modification of actin. *J. Biol. Chem.* 236:1338–1344.
54. Khan, A. U., and M. Kasha. 1979. Direct spectroscopic observation of singlet oxygen emission at 1268 nm excited by sensitizing dyes of biological interest in liquid solutions. *Proc. Natl. Acad. Sci. U.S.A.* 76:6047–6049.
55. Lin, T.-I. 1978. Fluorimetric studies of actin labeled with dansyl-aziridine. *Arch. Biochem. Biophys.* 185:285–299.
56. Knight, P., and G. Offer. 1978. p-NN'-phenylene-bis-maleimide, a specific cross-linking agent for F-actin. *Biochem. J.*, 175:1023–1032.
57. Oster, G., J. S. Bellin, R. W. Kimball, and M. E. Schrader. 1959. Dye-sensitized photooxidation. *J. Am. Chem. Soc.* 81:5095–5099.